Experimental study on the swelling behaviour of bentonite/claystone mixture

Qiong Wang, Anh Minh Tang, Yu-Jun Cui, Pierre Delage, Behrouz Gatmiri

▶ To cite this version:

HAL Id: hal-00655761

https://hal-enpc.archives-ouvertes.fr/hal-00655761

Submitted on 2 Jan 2012

Experimental study on the swelling behaviour of bentonite/claystone mixture

Qiong Wang[1], Anh Minh Tang[1], Yu-Jun Cui[1], Pierre Delage[1], Behrouz Gatmiri[2]

[1] Ecole des Ponts ParisTech, UR Navier/CERMES
[2] ANDRA, France

<u>Corresponding author:</u>
Prof. Yu-Jun CUI
Ecole des Ponts ParisTech
6-8 av. Blaise Pascal, Cité Descartes, Champs-sur-Marne
F-77455 MARNE LA VALLEE
France

Telephone : +33 1 64 15 35 50
Fax : +33 1 64 15 35 62
E-mail : yujun.cui@enpc.fr

Abstract

A mixture of the MX80 bentonite and the Callovo-Oxfordian (COx) claystone were investigated by carrying out a series of experiments including determination of the swelling pressure of compacted samples by constant-volume method, pre-swell method, zero-swell method and swell–consolidation method. Distilled water, synthetic water and humidity controlled vapour were employed for hydration. Results show that upon wetting the swelling pressure increases with decreasing suction; however, there are no obvious effects of synthetic water chemistry and hydration procedure on the swelling behaviour in both short and long terms. For the same initial dry density, the swelling pressure decreases with increasing pre-swell strain; whereas there is a well defined logarithmic relation between the swelling pressure and final dry density of the sample regardless of the initial dry densities and the experimental methods. It was also found that swelling pressure depends on the loading-wetting conditions as a consequence of the different microstructure changes occurred in different conditions. Furthermore, it was attempted to elaborate a general relationship between the swelling pressure and the final dry density for various reference bentonites.

Keywords: bentonite/claystone mixture; swelling pressure; water chemistry effect; long term behaviour; final density; correlation.

1 INTRODUCTION

Deep geological repository is being considered for high-level radioactive waste (HLW) in several countries such as China, Belgium, France, Germany, Japan, Sweden, etc. In most cases, compacted bentonite-based materials are chosen as sealing/buffer materials thanks to their low permeability, high swelling and high radionuclide retardation capacities (Pusch, 1979; Yong et al., 1986; Villar et al., 2008).

Once the repository is closed and local groundwater conditions are re-established, the water in the host rock formation will move to the repository. The bentonite-based material absorbs water and swells, filling the technical voids as the gaps between the bentonite bricks themselves, between the canister and the bricks, between bricks and the host rock, as well as the fractures in the host rock due to excavation. After that, the subsequent swelling is restrained by the host rock and swelling pressure develops. From a mechanical point of view, in order to ensure the stability of the system, the swelling pressure must be lower than the in situ minor stress: 7 MPa in the Underground Research Laboratory (URL) of Bure site, France (Delege et al., 2010; Tang et al., 2011a); 3-4 MPa at Tournemire site, France (Barnichon et al., 2009) and 4-5 MPa at Mol site, Belgium (Li et al., 2009), etc. As the compacted bentonite-based material is a key component of a repository system, it governs the overall behaviour of the whole system. Hence, a proper understanding of how the compacted bentonite-based material behaves during hydration process is essential for

62   the assessment of the short and long term performance of the repository system.

63   The behavior of compacted bentonite-based material upon wetting has been widely
64   investigated, in terms of swelling properties (Pusch, 1982; Komine and Ogata, 1994,
65   2003, 2004a; Delage et al., 1998; Agus and Schanz, 2005; Komine et al., 2009);
66   hydraulic behaviour under saturated state (Kenney et   al., 1992; Dixon et al., 1999;
67   Komine, 2004b;) and unsaturated state (Borgesson et al., 1985, 2001; Kröhn, 2003;
68   Lemaire el al., 2004; Loiseau et al., 2002; Cui et al., 2008). There are also many
69   studies on the effect of temperature (Komine and Ogata, 1998; Romero et al., 2001;
70   Villar and Lloret, 2004; Tang et al., 2005; Tang et al., 2007; Tang et al., 2008a; Tang
71   and Cui, 2009) and water chemistry of the saturating fluid (Pusch 2001a, Karland et
72   al., 2005; Suzuki et al., 2005; Komine et al., 2009) on the hydro-mechanical (HM)
73   behaviour.

74   For the swelling properties, it has been found that the swelling pressure determined
75   in the laboratory can be affected by the experimental methods (Sridharan et al., 1986;
76   Tang el al., 2011b). Normally, different methods give different values of swelling
77   pressure due to the difference in the loading and wetting conditions in each method
78   (Abdullah et al., 1998, 1999). In addition, the swelling properties depend on the
79   initial dry density and water content of the soil specimen. The higher the initial dry
80   density, the higher the swelling pressure or the higher the swelling strain; the
81   swelling strain decreases with increasing initial water content, but the swelling
82   pressure seems not to be affected by the initial water content (Komine et al., 1994;
83   Villar et al., 2008). The swelling properties can be also affected by the chemical
84   composition of the saturating fluid: the swelling capacity of the bentonite decreases
85   with the increase in salinity of saturating fluid, although this influence becomes less
86   significant for higher densities (Pusch, 1980; Sugita et al., 2003; Karnland et al.,
87   2005; Castellanos et al., 2008; Siddiqua et al., 2011). Moreover, studies on the aging
88   effects on the swelling behavior show that the swelling potential may decrease with
89   time due to the rearrangement of clay particles with time (Nalzeny et al., 1967; Day
90   et al., 1994; Subba Rao et al., 2003; Delage et al., 2006).

91   Very often, bentonite/sand mixtures are considered for the reasons of good control of
92   swelling pressure, large thermal conductivity and a better mechanical resistance. In
93   France, the mixture of bentonite and crushed Callovo-Oxfordian (COx) claystone
94   excavated from the Bure site of the ANDRA URL (-490 m, North-eastern France)
95   was proposed as a possible sealing and backfill material. This choice has several
96   advantages: (i) it is more economical by using local excavated claystone; (ii) the
97   negative impacts on the environment is reduced by recycling the excavated material;
98   (iii) there is better compatibility of mineralogical and chemical compositions with
99   host rock, allowing reduction of complex physico-chemical interaction with the host
100   rock (Andra, 2005; Tang et al., 2011a; Tang et al., 2011b). On the other hand, unlike
101   relatively inert sand, claystone contains clay minerals and interaction between
102   claystone and bentonite may occur, affecting the hydro-mechanical behaviour of the
103   compacted mixture. Moreover, this interaction can be of long term. Particular

104   attention should be paid to this aspect.

105   This study focuses on the swelling properties of the mixture MX80
106   bentonite/crushed Cox claystone. A series of swelling tests were performed under
107   constant temperature (20±1°C). The influences of water chemistry, hydration
108   procedure and duration, pre-existing technical void and loading-wetting paths on the
109   swelling pressure of compacted samples were investigated. Emphasis was put on the
110   relationship between the swelling pressure and the dry density of bentonite.

111

2 MATERIALS AND METHODS

113   2.1 Materials

114   The commercial MX80 bentonite from Wyoming, USA, was used. Table 1 lists its
115   physical parameters. It appears that the proportion of montmorillonite is dominant in
116   the bentonite (92 %); it has an average specific gravity of 2.76, a liquid limit of
117   520%, and a plastic limit of 42%. The grain size distribution determined by
118   sedimentation in Figure 1 shows that 84% grains are smaller than 2 µm (clay
119   fraction).

120   Callovo-Oxfordian (COx) claystone taken from the Bure site of the ANDRA URL
121   was studied. It contains 40–45% clay minerals (mainly interstratified minerals
122   illite–smectite), 20–30% carbonates and 20–30% quartz and feldspar (Hoteit et al.,
123   2000; Lebon and Ghoreychi, 2000; Zhang et al., 2004). The specific gravity is 2.70.
124   The excavated claystone was air-dried (w = 2.64%) and crushed to powder. The
125   grain size distribution determined by sedimentation is presented in Figure 1. It
126   confirms that 40% grains are clays (< 2 µm).
127   Both distilled water and synthetic water having the same chemical composition as
128   the site water (see Table 2) were used.

129   2.2 Samples preparation

130   All the tests in this study were performed on samples of compacted
131   bentonite/claystone mixture with a bentonite content of 70 % in dry mass. Bentonite
132   and claystone powders with the initial water contents of 11.8 % and 2.64 %
133   respectively, were used for the samples preparation. Their grain size distributions
134   were determined by sieving and are presented in Figure 1.

135   Samples were statically compacted in an oedometer cell (38 or 70 mm in internal
136   diameter) at a controlled rate of 0.05 mm/min. A load transducer was used for axial
137   force monitoring, and a micrometer dial gauge was used for axial displacement
138   monitoring. After compaction, the specimen was carefully transferred into the
139   hydration cell (with the same diameter as the oedometer cell) by connecting the
140   bottom of the two cells together. This procedure allows the lateral stress released
141   without significant increase in sample diameter.

142   2.3 Experimental methods

143   Various methods were used to determine the swelling pressure upon wetting. The
144   stress paths of these methods are presented in Figure 2.

145   For the "constant-volume" method (stress path OA), the devices presented in Figure
146   3 and Figure 4 were used. The constant-volume cell includes three parts (Figure 3,
147   Tang et al., 2011b): (1) the bottom part containing a porous stone and a drainage
148   system; (2) the middle cell (70 mm inner diameter) used to prevent radial swelling,
149   with two air outlets; (3) the top part incorporating a total pressure sensor to monitor
150   the swelling pressure. Figure 4 presents the setup used to control the suction in the
151   soil sample using the vapour equilibrium technique (see Delage et al., 1998 for more
152   details). When flooding the soil sample, this system was removed and the water inlet
153   was connected to a water reservoir.
154
155   For the "pre-swell" method (stress path OBB′), the sample was first allowed to swell
156   freely in the axial direction to a certain value (Point B, noted as "pre-swell"), then
157   the piston was fixed permitting the generation of swelling pressure that was
158   monitored by the load transducer. This method was used to investigate the effect of
159   pre-existing technical voids (simulated by the pre-swell allowed in the tests) on the
160   swelling pressure.

161   For the "zero-swell" and "swell-consolidation" methods, the equipment employed

162   was a conventional oedometer (Basma et al., 1995; Nagaraj et al., 2009). Firstly, a
163   low initial load of 0.1 MPa was exerted on the specimen prior to water flooding. As
164   the specimen wetted up it attempted to swell. When the swell exceeded 10 μm
165   (equivalent to 0.1%), additional pressure was added in small increment to bring the
166   volume of soil specimen back to its initial value (Basma et al., 1995; Abdullah et al.,
167   1998, 1999; Attom et al., 2001). This operation was repeated until the specimen
168   ceased to swell (OCC′ in Figure 2). The swelling pressure was defined as the stress
169   under which no more swelling strain was observed.

170   The "swell-consolidation" method consists of re-saturating the soil under a low
171   vertical pressure of 0.1 MPa until full swell was achieved. After swell completion,
172   standard consolidation test was conducted. The pressure required to compress the
173   specimen back to its original void ratio is defined as the swelling pressure (Basma et
174   al., 1995; Abdullah et al., 1998, 1999; Agus, 2005). The corresponding stress path
175   ODD′ is shown in Figure 2. In this path, point D also represents the maximum
176   swelling strain of the sample.

177   The experimental programme is shown in Table 3. Three tests were performed using
178   the constant-volume method to study the effect of water chemistry and the hydration
179   procedure (CV01, CV02 and CV03). Distilled water and synthetic water was used in
180   test CV01 and CV02, respectively. In test CV03, three suctions (57 MPa, 38 MPa

181 and 12.6 MPa) were first applied step by step using vapor equilibrium technique (as
182 shown in Figure 4), prior to distilled water flooding in the last stage.

183 Four tests were performed by pre-swell method to study the influence of pre-existing
184 technical voids on the swelling pressure (PS01 – PS04). Different pre-swells were
185 allowed before measurement of the swelling pressure. Note that for test PS04 the
186 sample was allowed to swell freely to reach the maximum pre-swell strain.
187
188 Two other tests were conducted using zero-swell method (ZSO1) and
189 swell-consolidation method (SCO1), respectively, for analyzing the influence of
190 loading-wetting paths followed in different experimental methods.
191
192 As it can be seen in Table 3, the tests conducted have in general long duration, from
193 80 h to one year.

194

195 **3 EXPERIMENTAL RESULTS**

196 Figure 5 presents the results from tests CV01 and CV02 with distilled water and
197 synthetic water respectively, during the first 100 h. The two curves are very similar,
198 showing negligible effect of water chemistry (in the range considered). With water
199 infiltration, swelling pressure increased first very quickly; after about 20 h the
200 swelling pressure reached a first stability stage. At 32 h, the swelling pressure
201 restarted to increase and it reached a second stability stage at 100 h. The final values
202 are 4.30 MPa and 4.37 MPa for CV01 and CV02, respectively.

203 The results of test CV03 is presented in Figure 6. The initial suction of sample was
204 about 90 MPa (measured by a relative humidity sensor on the soil specimen after the
205 compaction and prior to the installation in the cell). The application of the first
206 suction of 57 MPa resulted in a swelling pressure of 0.57 MPa. Then, the second
207 suction of 38 MPa was applied and the swelling pressure reached 1.43 MPa. With
208 the third suction of 12.6 MPa the swelling pressure increased to 2.61 MPa. The zero
209 suction applied by distilled water led the sample to a maximum value of 4.39 MPa
210 swelling pressure. This value is very close to that from test CV01 (4.30 MPa) and
211 CV02 (4.37 MPa) in which the samples were flooded directly with water. This
212 means there is no kinematic effect on the swelling pressure for the studied mixture.

213 Figure 7 presents the relationship between the swelling pressure (σ_s in MPa) and the
214 suction (s in MPa), with the values obtained from test CV03. An exponential
215 function can be used to satisfactorily describe this relationship:

216 $$\sigma_s = 4.9908 \times 10^{-0.0178s} \qquad \text{(Eq.1)}$$

217 In Figure 8, the whole results from the three tests CV01, CV02 and CV03 during one
218 year are presented. It appears that after a long period of one year, there was just a

slight decrease of swelling pressure and the values for the three samples still remain very close (4.23MPa, 4.32MPa and 4.29MPa for test CV01, CV02 and CV03, respectively). This shows a negligible effect of any bentonite-claystone interaction on the swelling pressure.

The evolution of swelling pressure for the specimens having the same initial dry density of 1.90 Mg/m^3 with different pre-swells is presented in Figure 9. An expected significant decrease of swelling pressure with increasing pre-swell is observed. For the pre-swells of 10, 20 and 25%, the swelling pressures obtained are 5.38, 2.03 and 0.7 MPa, respectively. Note that the maximum swelling strain from test PS04 reaches 43 %.

The results from test SCO1 using the swell-consolidation method are presented in Figure 10. When wetting up, the sample swelled under a low vertical pressure of 0.1 MPa and the maximum swelling strain reached 41.76%. Further compression gave a normal consolidation curve that allows the determination of the swelling pressure: $\sigma_s = 22.20$ MPa.

For test ZSO1 (zero-swell method) on a sample at an initial dry density of 1.70 Mg/m^3, a vertical stress of 4.38 MPa was needed to keep the void radio constant. By definition, this value is the swelling pressure by this method.

From the results in Figure 9, the swelling pressure is plotted versus the pre-swell strain in Figure 11. The maximum pre-swell of test PS04 and the swelling strain in SCO1 (swell consolidation method) are also presented in this figure. Note that all specimens had the same initial dry density of 1.90 Mg/m^3 and all flooded with synthetic water. It appears that the result of SCO1 is close to that of PS04 (free swell), showing a good repeatability of the free-swell tests. A linear correlation can be obtained between the swelling strain allowed (ε in %) and the logarithm of swelling pressure (σ_s in MPa):

$$\varepsilon = -19.32 Lg(\sigma_s) + 23.946 \qquad \text{(Eq.2)}$$

In Figure 12, the swelling pressure determined by the pre-swell method (PS01, PS02, PS03, PS04), constant-volume method (CV02), zero swell method (ZSO1) are plotted in the plane of void ratio/logarithm of vertical stress, together with the consolidation line from test SCO1. Point O and O′ correspond to the initial states of the samples at a dry density of 1.90 Mg/m^3 (PS01, PS02, PS03, PS04 and SCO1) and 1.70 Mg/m^3 (CV02 and ZSO1), respectively. It can be noted that at the same void ratio, the vertical stress of the consolidation curve (SCO1) is slightly higher than the swelling pressure determined by other methods.

Figure 13 shows the measured swelling pressure versus the final dry density of the bentonite/claystone mixture for all the tests. Note that these tests have been performed with two different initial dry densities ($\rho_{di} = 1.90$ Mg/m^3 for tests PS01,

257 PS02, PS03, PS04, SCO1; and ρ_{di} = 1.70 Mg/m³ for tests CV02, ZSO1), and using
258 various methods (see Table 3). In spite of this, a unique correlation seems enough to
259 describe the relationship between the swelling pressure σ_s (MPa) and the final dry
260 density of the mixture ρ_{dm} (Mg/m³):

261
$$\sigma_s = 4.8 \times 10^{-7} \exp^{9.41\rho_{dm}}$$
Eq.3

262 This shows that the swelling pressure of the compacted claystone/bentonite mixture
263 is mainly dependent on the final dry density of the mixture. For a deeper analysis on
264 the role of the bentonite itself in the swelling pressure development of the bentonite-
265 based mixutre, the dry density of bentonite (ρ_{db}) was considered by assuming that the
266 water content of additives (claystone in this study) kept constant, while the water
267 added during the tests was totally absorbed by bentonite. The volume of bentonite
268 (V_b) is the difference between the total volume (V) and the volume of claystone (soil
269 particles and water inside). The bentonite dry density can be calculated by the
270 following equation:

271
$$\rho_{db} = \frac{(B/100)\rho_m G_{sa}}{G_{sa}(1 + w_m/100) - \rho_m(1 - B/100)(1 + w_a)}$$
(Eq.4)

272 where ρ_m (Mg/m³) is the mixture density; B (%) is the bentonite content (in dry mass)
273 in the mixture; w_m is the water content of the mixture; w_a is the initial water content
274 of claystone; G_{sa} is the specific gravity of claystone. In this study, w_a = 2.64%, B =
275 70 %, G_{sa} = 2.70.

276 Using Eq. 4, the results shown in Figure 13 were re-analysed and Figure 15 shows
277 the variations of swelling pressure with the final dry density of bentonite. In the
278 same figure, the results collected from other works on the MX80/sand mixture
279 (Karland et al., 2008) and the pure MX80 bentonite (Karnland et al., 2008; Dixon et
280 al., 1996) are also presented. A very similar relationship is obtained for the different
281 data sets, showing that the swelling pressure mainly depends on the final dry density
282 of bentonite, sand and claystone being both inactive components in the mixtures for
283 the swelling pressure development.
284
285 To further investigate this point, results on other reference bentonites were collected
286 and analysed in the same fashion. Figure 15 shows the variations of swelling
287 pressure with the final dry density of MX80 (from Figure 14), FoCa7 (Imbert et al.,
288 2006), FEBEX (Villar et al., 2002) and Kunigel V1 (Dixon et al., 1996). It appears
289 that for each bentonite, there is a unique relationship between the swelling pressure
290 and the final dry density of bentonite. However, the relationships are not the same. A
291 general expression can be proposed:

292
$$\sigma_s = \alpha \times \exp^{\beta\rho_{db}}$$
Eq.5

293 where α and β are the two constants.
294

Table 4 shows the values of α and β for the four bentonites analysed. In the table, the mineralogy of these materials is also presented. The difference of parameters can be related to the different types of clay (i.e. montmorillonite, beidellite and saponite, etc), montmorillonite content and type of exchangeable cations (i.e. calcium or sodium). In general, the swelling capacity of sodium bentonite is higher than that of calcium bentonite; with the same type of exchangeable cations, a larger montmorillonite content leads to a higher swelling pressure.

5 DISCUSSION

It has been observed that the effect of the chemistry of Bure site water on the swelling pressure is negligible. However, it is generally accepted that the swelling pressure decreases with the increase in salinity of the pore-water, although this decrease becomes less significant in case of high density (Karnland et al., 2005; Castellanos et al., 2008; Siddiqua et al., 2011; Komine et al., 2009). Castellanos et al. (2008) reported that the swelling pressure of the FEBEX bentonite compacted to a dry density of 1.65 g/cm^3 decreases to almost half its initial value when 2 mol/L CaCl$_2$ and NaCl/L solutions are used as saturating fluids; At low salinities (0.004 mol/L, granitic water), the swelling pressure of bentonite seems not to be affected by the salinity changes at a dry density ranging from 1.40 to 1.70 Mg/m^3. It appears that for the studied bentonite/claystone mixture, the high density and the low salinity of synthetic water together resulted in the negligible effect of water chemistry on the swelling pressure. This can be explained by the theory of cations filtration (Komine et al., 2009). For high dry density of bentonite-based materials, the distances between the montmorillonite mineral layers being very small, these layers can filter the cations in the solution; on the contrary, in the case of low dry density, the cations in solution can infiltrate easily into the montmorillonite mineral layers due to the larger distances between them, thus affecting the swelling behaviour.

For the sample wetted with suction control (CV03), an exponential function was found between the swelling pressure and the suction applied. This can be explained as follows. As clay samples are exposed to humid water vapour, water molecules first migrate into the open channels and adsorbed on the exposed mineral surface (Pusch, 2001b; Arifin, 2008), then move to elementary clay layers. The number of water molecules absorbed by the clay layers depends on the relative humidity or suction (Pusch, 2001b; Saiyouri et al., 2004; Delage, 2006), and this number of water molecules defines the swelling pressure of the sample. Therefore the swelling pressure is suction or relative humidity dependent. After the sample was flooded with distilled water, the maximum swelling pressure was found close to that obtained by water-flooding the sample directly, indicating the negligible effect of wetting procedure. This phenomenon can be explained by the mechanism identified by Cui et al. (2002): when hydrating by decreasing suction (57-38-12.6 MPa) under confined conditions, the size of macro-pores was progressively decreased, whereas the micro-pores remained almost un-affected. The micro-pores started to change

337   only when the water saturation is approached. This suggests that step-wetting by
338   suction control and direct saturation by water flooding may lead to similar final
339   microstructures, thus similar final swelling pressures.

340   Yang et al. (2008) reported that the mineralogical composition of the bentonite will
341   not be stable under the chemistry fluid infiltration and its properties may degrade
342   over long time periods. Moreover, for the bentonite/claystone mixture used in this
343   study, interaction of claystone with water and bentonite was suspected. This justifies
344   the long swelling tests kept over one year. However, no any significant effects were
345   observed on the swelling pressure. It is possible that one year test is not long enough
346   and this point should be studied further with longer tests, giving the long-term nature
347   of the nuclear waste disposal.

348   A linear correlation was observed between the pre-swelling strain and the logarithm of
349   swelling pressure for the samples with the same initial dry density. This line defines
350   the limit of swelling potential: the samples at the same initial state followed different
351   stress-volume paths until reached this limit and then no further expansion occurred.
352   This is consistent with the conclusion of Villar et al. (2008) and Siemens et al. (2009)
353   who found a similar relationship between swelling strain and swelling pressure. It can
354   be seen that the final state of specimen governed the swelling pressure: for the
355   samples with the same initial state, different pre-swelling strains led to different final
356   dry densities and thus resulted in different swelling pressure. Moreover, a unique
357   relationship was observed between the swelling pressure and the final dry density of
358   the samples whatever the initial dry density, the percentage of pre-swell and the
359   experimental method. This also enhances the conclusion that the final state of the
360   sample controls the swelling pressure. Further analysis showed that the swelling
361   pressure mainly depends on the final dry density of bentonite in the mixture. This
362   observation is in agreement with the conclusion of Lee et al. (1999) and Agus (2005)
363   who noted that the swelling pressure of bentonite/sand mixtures with different
364   bentonite contents is a function of the final bentonite dry density. This suggests that
365   the swelling mechanism of bentonite-based materials is the same as that of pure
366   bentonites.

367   At the same void ratio, the swelling pressure determined by different methods was
368   found slightly lower than the vertical stress needed to reach the same void ratio
369   following the swell-reload path (swell-consolidation method). This was in agreement
370   with the results by many other authors (Justo et al., 1984; Sridharan et al., 1986;
371   Basma et al., 1995; Abdullah et al., 1998, 1999; Agus, 2005; Villar, 1999; Villar et al.,
372   2008), and can be considered as a consequence of the coupling between the
373   microstructure and macrostructure (Gens and Alonso, 1992; Villar, 1999; Sánchez et
374   al., 2005). For the swell-consolidation oedometer test, wetting took place under a low
375   vertical load and the void ratio increased greatly due to the large microstructural
376   changes. In this case, intense breakage of particle aggregates occurs, leading to
377   relatively uniform distribution of the expandable component. A relatively high
378   vertical stress was needed to compensate this large macrostructure deformation. By

379 contrast, smaller microstructure and macrostructure interaction is expected in other
380 methods, with lower stress at full saturation. Furthermore, the relative larger
381 displacement in the swell-consolidation oedometer test would mobilise higher friction
382 and this friction can also contribute to the phenomenon observed.
383

384 ## 6 CONCLUSION

385 The swelling pressure of bentonite/claystone mixture was determined by different
386 methods. The effects of the water chemistry, the hydration procedure, the
387 pre-existing technical voids and the experimental methods on the swelling pressure
388 were investigated. From the experimental results the following conclusion can be
389 drawn.

390 There was no obvious effect of water chemistry on the swelling pressure due to the
391 high density and the low salinity of synthetic water.

392 An exponential function was found between the swelling pressure and the suction
393 applied; no effect of hydration procedure on the final swelling pressure was observed.

394 The swell-consolidation method gives higher swelling pressure mainly because of
395 the coupling between the microstructure deformation and macrostructure
396 deformation. The effect of friction is also to be considered for this phenomenon.

397 The swelling pressure of bentonite-based materials mainly depends on the final dry
398 density of the bentonite in the mixture, suggesting that the swelling mechanism of
399 bentonite-based materials is the same as that of pure bentonites. A general relationship
400 between the swelling pressure and the final dry density of various bentonites was
401 proposed, with two parameters depending on the montmorillonite content and the type
402 of exchangeable cations.

403 From a practical point of view, the relationship elaborated between the swelling
404 pressure and the final bentonite dry density is helpful in designing the sealing/filling
405 buffers with bentonite-based materials: when the initial state of bentonite-based
406 materials and the technical voids are known, the final swelling pressure can be
407 predicted. Moreover, the crushed Cox claystone can be used to form the
408 bentonite/claystone mixture because it behaves as sand. However it should be noted
409 that this conclusion is based on the results from one year tests and further studies with
410 longer tests are needed to gain more confidence on this aspect.

411

7 REFERENCE

Abdullah, I., Mhaidib, A., 1998. Prediction of swelling potential of an expansive shale. Proceedings Of The Second International Conference On unsaturated soils. 27-30 August. Beijing, China: vol. 1.

Abdullah, I., Mhaidib, A.l., 1999. Swelling behaviour of expansive shales from the middle region of Saudi Arabia. Geotechnical and Geological Engineering. 16(4):291–307.

Agus, S., 2005. An Experimental study on hydro-mechanical characteristics of compacted bentonite-sand mixtures. PhD thesis. Weimar.

Agus, S., Schanz, T., 2005. Swelling pressures and wetting-drying curves of a highly compacted bentonite-sand mixture. Unsaturated Soils: Experimental Studies, pages 241–256.

Andra, 2005. Référentiel des matériaux d'un stockage de déchets à haute activité et à vie longue – Tome 4: Les matériaux à base d'argilites excavées et remaniées. Rapport Andra N° CRPASCM040015B.

Arifin, Y.F., 2008. Thermo-hydro-mechanical behavior of compacted bentonite sand mixtures: An Experimental Study. PhD thesis. Weimar.

Attom, M.; Abu-Zreig, M. & Obaidat, M. 2001. Changes in clay swelling and shear strength properties with different sample preparation techniques. ASTM geotechnical testing journal, ASTM, 24, 157-163.

Barnichon, J.D., and Deleruyelle, F., 2009. Sealing Experiments at the Tournemire URL. Towards convergence of technical nuclear safety practices in Europe, EUROSAFE.

Basma,A.A., Al-Homoud, A.S., Husein, A., 1995. Laboratory assessment of swelling pressure of expansive soils. Applied Clay Science, 9(5):355–368.

Borgesson, L. 1985. Water flow and swelling pressure in non-saturated bentonite-based clay barriers. Engineering Geology, 21(3-4):229–237.

Borgesson, L., Chijimatsu, M., Fujita,T., Nguyen, T.S., Rutqvist, J., Jing, L., 2001. Thermo-hydro-mechanical characterisation of a bentonite-based buffer material by laboratory tests and numerical back analyses. International Journal of Rock Mechanics and Mining Sciences, 38(1):95–104.

Castellanos, E., Villar, M.V., Romero, E., Lloret, A., Gens, A., 2008. Chemical impact on the hydro-mechanical behaviour of high-density febex bentonite. Physics and Chemistry of the Earth, Parts A/B/C, 33(Supplement 1):S516 – S526.

Cui, Y. J., Loiseau, C., Delage, P., 2002. Microstructure changes of a confined swelling soil due to suction controlled hydration Unsaturated soils: proceedings of the Third International Conference on Unsaturated Soils, UNSAT 2002, 10-13 March 2002, Recife, Brazil, 593.

Cui, Y.J., Tang, A.M., Loiseau, C., Delage, P., 2008. Determining the unsaturated hydraulic conductivity of a compacted sand-bentonite mixture under constant-volume and free-swell conditions. Physics and Chemistry of the Earth, Parts A/B/C, 33(Supplement 1): 462 – S471.

Day, R.W. 1994. Swell-shrink behaviour of expansive compacted clay. J. Geotechnical

461   Engneering, ASCE 120, No. 3, 618–623.

462   Delage, P., Howat, M. D. & Cui, Y. J., 1998. The relationship between suction and swelling

463   properties in a heavily compacted unsaturated clay. Engineering Geology 50**,** 31-48.

464   Delage, P., Marcial, D., Cui, Y.J., and Ruiz, X., 2006. Ageing effects in a compacted

465   bentonite: a microstructure approach. Geotechnique, 56(5):291–304.

466   Delage, P. 2006. Some microstructure effects on the behaviour of compacted swelling clays

467   used for engineered barriers. Chinese Journal of Rock Mechanics and Engineering,

468   Science Press(Beijing), 16 Donghuangchenggen North St, Beijing, 100717, China,, 25,

469   721-732.

470   Delage, P., Cui, Y.J., Tang, A.M., 2010. Clays in radioactive waste disposal, Journal of Rock

471   Mechanics and Geotechnical Engineering, Vol (2):111–123.

472   Dixon, D.A., Gray, M.N., Graham, J., 1996. Swelling and hydraulic properties of bentonites

473   from Japan, Canada and USA. In Proceedings of the second International Congress on

474   Environmental Geotechnics, Osaka, Japan, pages 5–8.

475   Dixon, D.A., Graham, J., and Gray, M.N., 1999. Hydraulic conductivity of clays in confined

476   tests under low hydraulic gradients. Canadian Geotechnical Journal, 36(5):815–825.

477   Gens, A., Alonso, E.E. 1992. A framework for the behaviour of unsaturated expansive clays.

478   Canadian Geotechnical Journal, 29(6):1013–1032.

479   Hoteit N, Ozanam-O, Su, K. 2000. Geological radioactive waste disposal project in france-

480   conceptual model of a deep geological formation and underground research laboratory

481   in Meuse Haute-Marne site. In The 4th North American Rock Mechanics Symposium,

482   Seattle, July 31-August 3.

483   Imbert, C., and Villar, M.V., 2006. Hydro-mechanical response of a bentonite pellets-powder

484   mixture upon infiltration. Applied Clay Science, 32(3-4):197–209.

485   Justo, J.L., Delgado, A., Ruiz, J., 1984. The influence of stress-path in the collapse-swelling

486   of soils at the laboratory. In Fifth International Conference on Expansive Soils 1984.

487   Australia. Page 67.

488   Karnland, O., Muurinen, A., Karlsson, F., 2005. Bentonite swelling pressure in NaCl

489   solutions-Experimentally determined data and model calculations. Advances in

490   Understanding Engineering Clay Barriers. Page 241.

491   Karnland, O., Nilsson, U., Weber, H., and Wersin, P., 2008. Sealing ability of Wyoming

492   bentonite pellets foreseen as buffer material-Laboratory results. Physics and Chemistry

493   of the Earth, Parts A/B/C, 33:S472–S475.

494   Kenney, T.C., Veen, W.A.V., MA Swallow, and Sungaila., M.A., 1992. Hydraulic

495   conductivity of compacted bentonite-sand mixtures. Canadian Geotechnical Journal,

496   29(3):364–374.

497   Komine., H., Ogata, N. 1994. Experimental study on swelling characteristics of compacted

498   bentonite. Canadian geotechnical journal, 31(4):478–490.

499   Komine., H., Ogata, N. 1998. Thermal influence on compacted bentonite for nuclear waste

500   disposal. In Proceedings of the 3rd International Congress on Environmental

501   Geotechnics, volume 1, pages 34–39.

502   Komine., H., Ogata, N. 2003. New equations for swelling characteristics of bentonite-based

503   buffer materials. Canadian Geotechnical Journal, 40(2):460–475.

504   Komine., H., Ogata, N. 2004a. Predicting swelling characteristics of bentonites. Journal of

505   Geotechnical and Geoenvironmental engineering, 130:818.

506   Komine, H., 2004b. Simplified evaluation for swelling characteristics of bentonites,
507   Engineering geology, 71(3-4): 265-279.

508   Komine, H. Yasuhara, K. and Murakami, S. 2009. Swelling characteristics of bentonites in
509   artificial seawater. Canadian Geotechnical Journal, 46(2):177-189.

510   Kröhn, K.P. 2003. Results and interpretation of bentonite resaturation experiments with
511   liquid water and water vapour. In: Schanz, T. (Ed.), Proceedings of the International
512   Conference from Experimental Evidence towards Numerical Modeling of Unsaturated
513   Soils, Weimar, Germany, vol. 1. 598 Springer, Berlin, pp. 257–272.

514   Lebon, P. and Ghoreychi, M. 2000. French underground research laboratory of Meuse,
515   Haute-Marne THM aspects of argillite formation. In Eurock 2000 Symposium, March,
516   pages 27–31.

517   Lee, J.O., Cho, W.J. and Chun, K.S., 1999. Swelling Pressures of a Potential Buffer Material
518   for High-Level Waste Repository. Journal of the Korean Nuclear Society, 31: 139-150.

519   Lemaire, T., Moyne, C., and Stemmelen, D., 2004. Imbibition test in a clay powder (MX-80
520   bentonite). Applied Clay Science, 26(1-4):235–248.

521   Li, X.L., Bastiaens, W., Van Marcke, P., et al., 2009. Design and Development of the Large
522   Scale In-situ PRACLAY Heater Test and Horizontal HLW Disposal Gallery Seal Test in
523   Belgian URL Hades,International Symposium on Unsaturated Soil Mechanics and
524   Deep Geological Nuclear Waste Disposal , Shanghai, China: 24—28.

525   Loiseau, C., Cui, Y.J. and Delage, P., 2002. The gradient effect on the water flow through a
526   compacted swelling soil, In: Proc. 3rd Int Conf Unsaturated Soils, UNSAT 2002, Recife,

527   Brazil, Balkema 1:395–400.

528   Nagaraj, H.; MOHAMMED Munnas, M.; Sridharan,A., 2009. Critical Evaluation of
529   Determining Swelling Pressure by Swell-Load Method and Constant Volume Method,
530   ASTM geotechnical testing journal, ASTM, 32, 305-314.

531   Nalezny, C. L. & Li, M. C., 1967. Effects of soil moisture and thixotropic hardening on the
532   swell behaviour of compacted expansive soils. Highway Res. Rec. Washington, DC:
533   Highway Research Board. No. 209.

534   Pusch, R., 1979. Highly compacted sodium bentonite for isolating rock-deposited
535   radioactive waste products. Nucl. Technol, United States. 45(2):153-157.

536   Pusch, R. 1980. Swelling pressure of highly compacted bentonite. SKBF/KBS technical
537   report: No.80-13.

538   Pusch, R., 1982. Mineral-water interactions and their influence on the physical behavior of
539   highly compacted Na bentonite. Canadian Geotechnical Journal, 19(3):381–387.

540   Pusch, R., 2001a. Experimental study of the effect of high porewater salinity on the physical
541   properties of a natural smectitic clay, SKBF/KBS technical report. No.TR01-07.

542   Pusch, R. 2001b. The microstructure of MX-80 clay with respect to its bulk physical
543   properties under different environmental conditions, SKBF/KBS technical report.
544   No.TR01-08.

545   Romero, E., Gens, A., and Lloret, A., 2001. Temperature effects on the hydraulic behaviour
546   of an unsaturated clay. Geotechnical and Geological Engineering, 19(3):311–332.

547   Saiyouri, N., Tessier, D., and Hicher, P.Y., 2004. Experimental study of swelling in

548   unsaturated compacted clays. Clay Minerals, 39(4):469.

549 Sanchez, M., Gens, A., Do Nascimento Guimarães, L., Olivella, S., 2005. A double structure
550   generalized plasticity model for expansive materials. International Journal for
551   Numerical and Analytical Methods in Geomechanics, 29(8):751–787.

552 Siddiqua, S.; Blatz, J. & Siemens, G.. 2011. Evaluation of the impact of pore fluid chemistry
553   on the hydromechanical behaviour of clay-based sealing materials. Canadian
554   Geotechnical Journal, NRC Research Press, 48, 199-213.

555 Siemens, G., and Blatz, J.A., 2009. Evaluation of the influence of boundary confinement on
556   the behaviour of unsaturated swelling clay soils. Canadian Geotechnical Journal,
557   46(3):339–356.

558 Sridharan, A., Rao, S., Sivapullaiah, P.V., 1986. Swelling pressure of clays. ASTM
559   geotechnical testing journal, 9(1):24–33.

560 Sugita, Y., Chijimatsu, M., and Suzuki, H., 2005. Fundamental properties of bentonite pellet
561   for Prototype Repository Project. Advances in Understanding Engineering Clay
562   Barriers, page 293.

563 Suzuki, S.; Prayongphan, S.; Ichikawa, Y. & Chae, B. 2005. In situ observations of the
564   swelling of bentonite aggregates in NaCl solution, Applied Clay Science, Elsevier, 29:
565   89-98.

566 Subba Rao, K. S. & Tripathy, S. 2003. Effect of aging on swelling and swell-shrink behaviour
567   of a compacted expansive soil. ASTM Geotech. Test. J. 26, No. 1, 36–46.

568 Tang, A.M., Cui, Y.J., 2005. Controlling suction by the vapour equilibrium technique at
569   different temperatures and its application in determining the water retention properties
570   of MX80 clay. Canadian Geotechnical Journal, 42 (1): 287-296.

571 Tang, A.M., Cui, Y.J., Barnel, N., 2007. A new isotropic cell for studying the
572   thermo-mechanical behavior of unsaturated expansive soil. Geotechnical Testing
573   Journal, 30 (5): 341 – 348.

574 Tang, A.M., Cui, Y.J., Barnel, N., 2008a. Thermo-mechanical behaviour of a compacted
575   swelling clay. Géotechnique, 58 (1): 45-54.

576 Tang, A.M., Cui, Y.J., Le, T.T., 2008b. A study on the thermal conductivity of compacted
577   bentonites. Applied Clay Science, 41 (3-4): 181 – 189.

578 Tang, A.M., Cui, Y.J., 2009. Modelling the thermo-mechanical behaviour of compacted
579   expansive clays. Géotechnique, 59 (3): 185-195.

580 Tang, C.S., Tang, A.M., Cui, Y.J., Delage, P., Barnichon, J.D., Shi, B., 2011a. A study of the
581   hydro-mechanical behaviour of compacted crushed argillite. Engineering Geology. 118
582   (3-4):93-103.

583 Tang, C.S., Tang,A.M., Cui, Y.J., Delage, P., Schroeder, C., De Laure, E., 2011b.
584   Investigating the Swelling Pressure of Compacted Crushed-Callovo-Oxfordian Argillite.
585   Physics and Chemistry of the Earth. (accepted)

586 Villar, M.V., Lloret, A., 2004. Influence of temperature on the hydro-mechanical behaviour
587   of a compacted bentonite. Applied Clay Science, 26(1-4):337 – 350.

588 Villar, M.V., 1999. Investigation of the behaviour of bentonite by means of
589   suction-controlled oedometer tests. Engineering Geology, 54(1-2):67–73.

590 Villar, M.V., 2002. Thermo-hydro-mechanical characterisation of a bentonite from Cabo de
591   Gata. A study applied to the use of bentonite as sealing material in high level

592   radioactive waste repositories. Publicación Técnica ENRESA 01/2002, Madrid, 258 pp.

593 Villar, M.V., Lloret, A., 2008. Influence of dry density and water content on the swelling of a

594   compacted bentonite. Applied Clay Science, 39(1-2):38–49.

595 Yang, J., Samper, C., and Montenegro, L., 2008. A coupled non-isothermal reactive transport

596   model for long-term geochemical evolution of a HLW repository in clay.

597   Environmental Geology, 53(8):1627–1638.

598 Yong, R.N., Boonsinsuk, P., and Wong, G., 1986.Formulation of backfill material for a

599   nuclear fuel waste disposal vault. Canadian Geotechnical Journal, 23(2):216–228.

600 Zhang, C., and Rothfuchs, T., 2004. Experimental study of the hydro-mechanical behaviour

601   of the Callovo-Oxfordian argillite. Applied Clay Science, 26(1-4):325–336.

624

Table 1 Characteristics of MX80 bentonite (Tang et al., 2008b)

Montmorillonite (%)	92
Quartz (%)	3
w_l (%)	520
w_p (%)	42
I_p	478
ρ_s (Mg/m^3)	2.76

Table 2 Chemical components of the synthetic water

Components	$NaHCO_3$	Na_2SO_4	NaCl	KCl	$CaCl_2.2H_2O$	$MgCl_2.6H_2O$	$SrCl_2.6H_2O$
Mass (g) per 1L solution	0.28	2.216	0.615	0.075	1.082	1.356	0.053

Table 3 Test programme

Test No.	Injected water	Method	Initial dry density (Mg/m^3)	Duration
CV01	Distilled	Constant-volume	1.70	1 year
CV02	Synthetic	Constant-volume	1.70	1 year
CV03	Vapour and distilled	Constant-volume	1.70	1 year
PS01	Synthetic	Pre-swell $\varepsilon = 10\%$	1.90	100 h
PS02	Synthetic	Pre-swell $\varepsilon = 20\%$	1.90	100 h
PS03	Synthetic	Pre-swell $\varepsilon = 25\%$	1.90	100 h
PS04	Synthetic	Pre- swell $\varepsilon = $ max	1.90	80 h
ZSO1	Synthetic	Zero-swell	1.70	80 h
SCO1	Synthetic	Swell-consolidation	1.90	4 months

Table 4 Montmorillonite content and external cations type of several bentonites

Bentonite	α	β	Montmorillonite Content (%)	Type
MX 80	1.78×10^{-4}	6.75	75-90	Na
FEBEX	9.80×10^{-5}	6.85	92	Ca
FoCa	7.83×10^{-7}	9.24	50 Beidellite 50 Kaollite	Ca
Kunigel V1	3.67×10^{-3}	3.32	48	Na
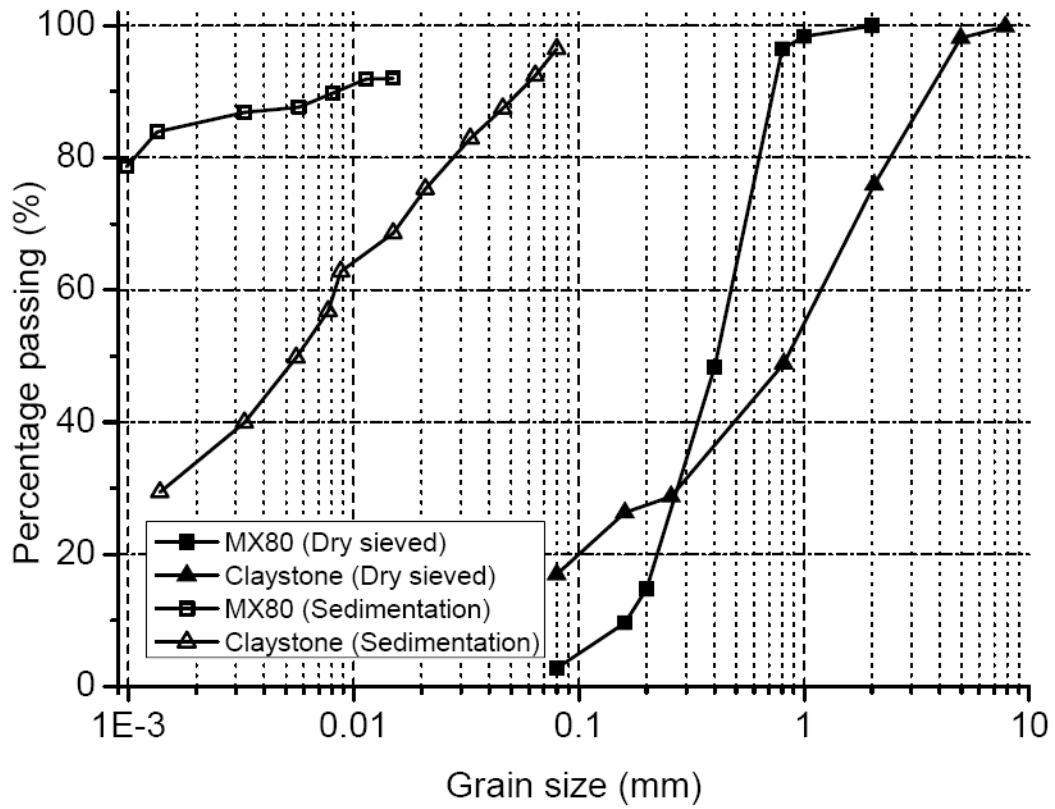
Figure 1. Grain size distribution of MX80 bentonite and crushed COx claystone
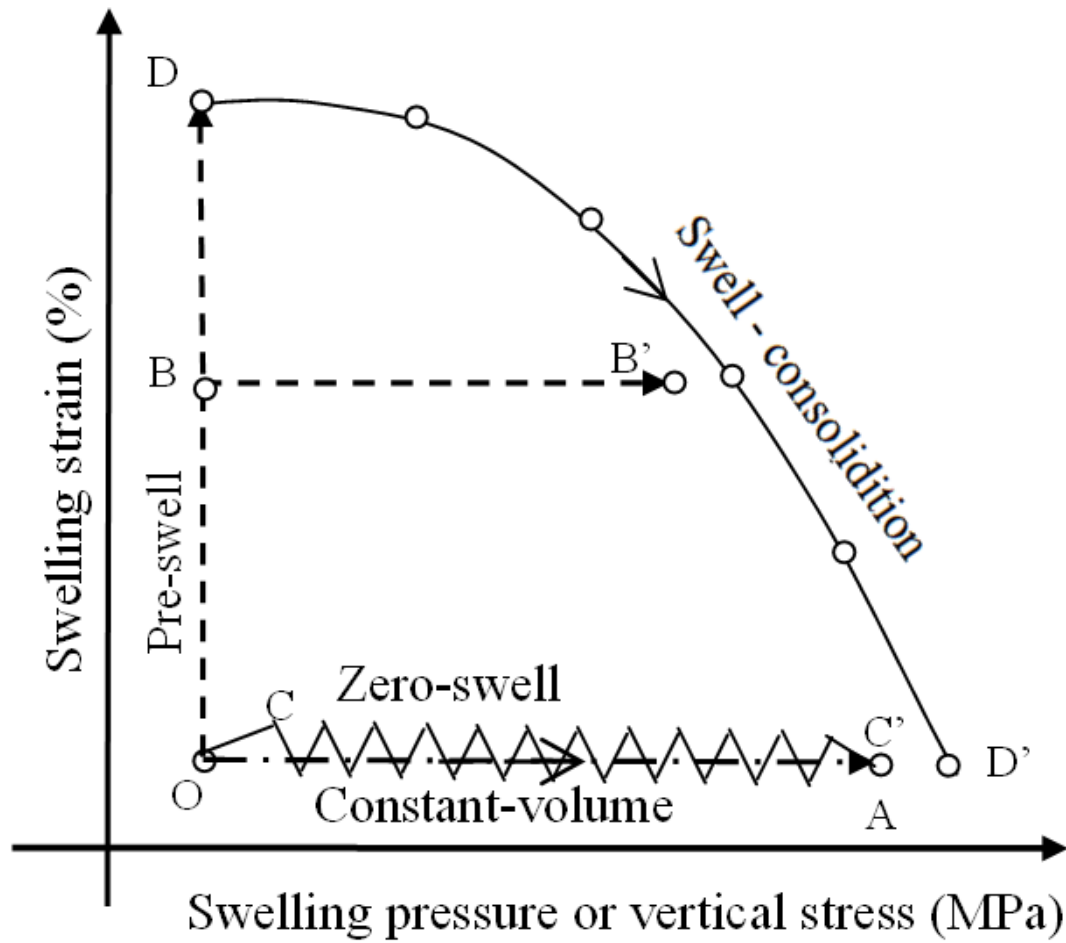
Figure 2. Stress path of various experimental methods used to determine the swelling pressure
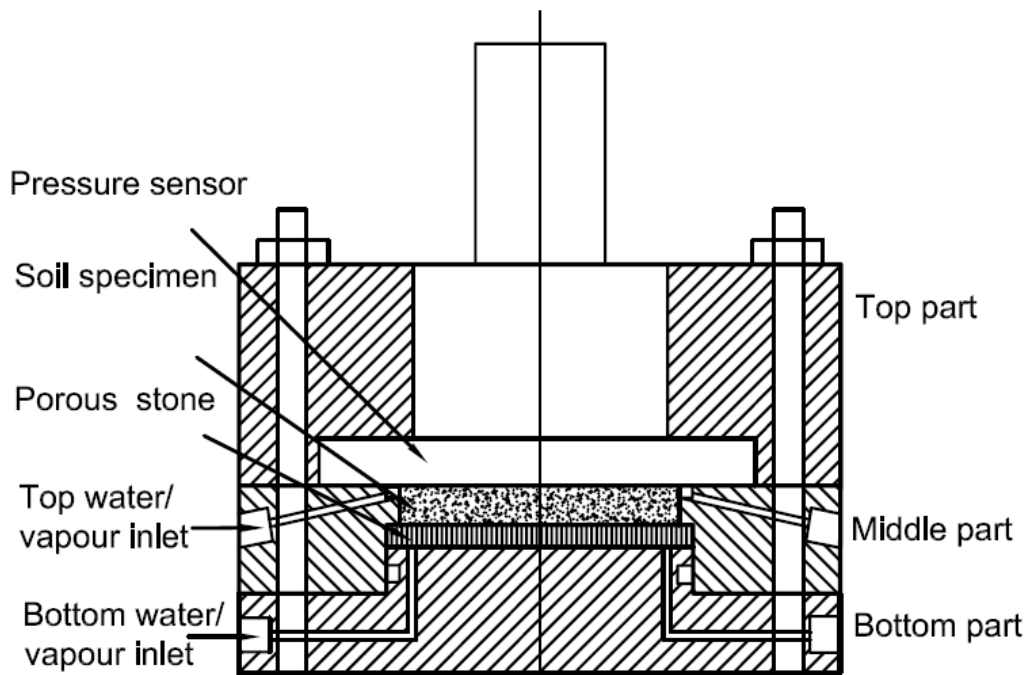
Figure 3. Constant-volume cell
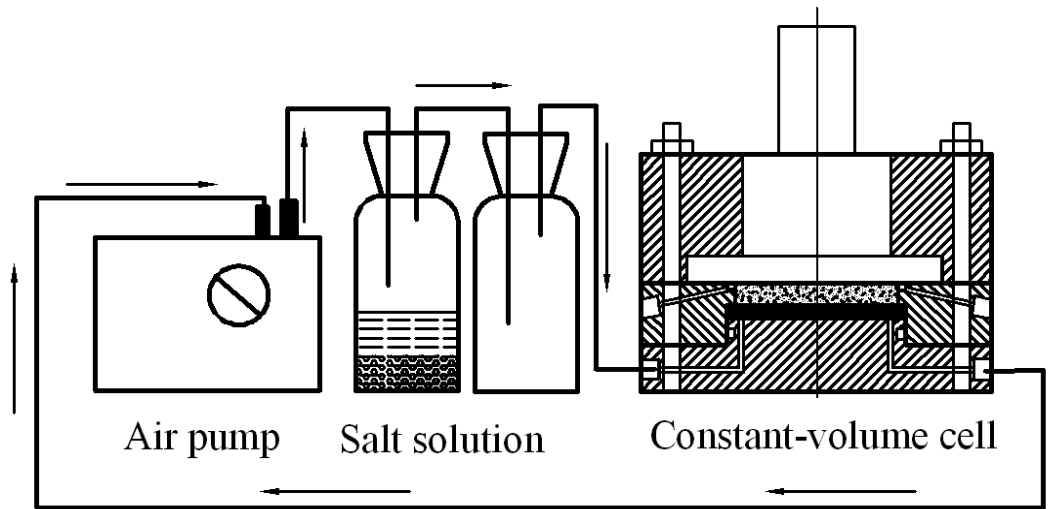
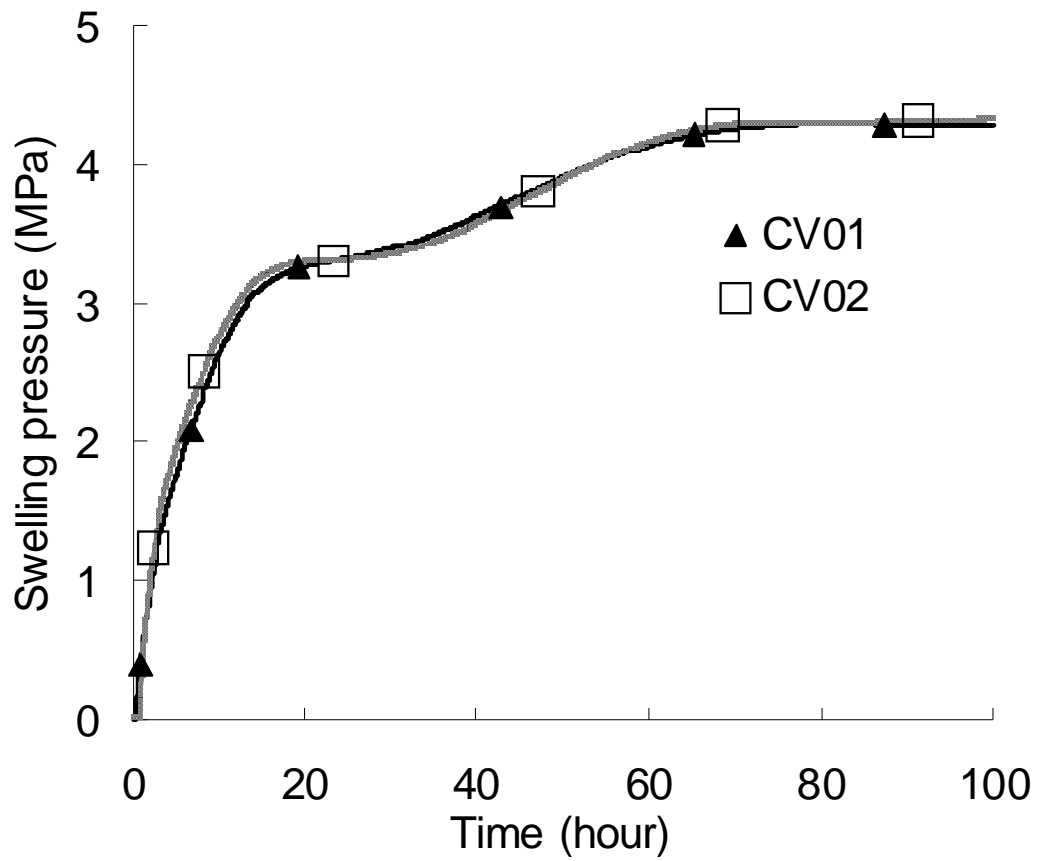Figure 4. Schematic view of constant volume cell with suction control system

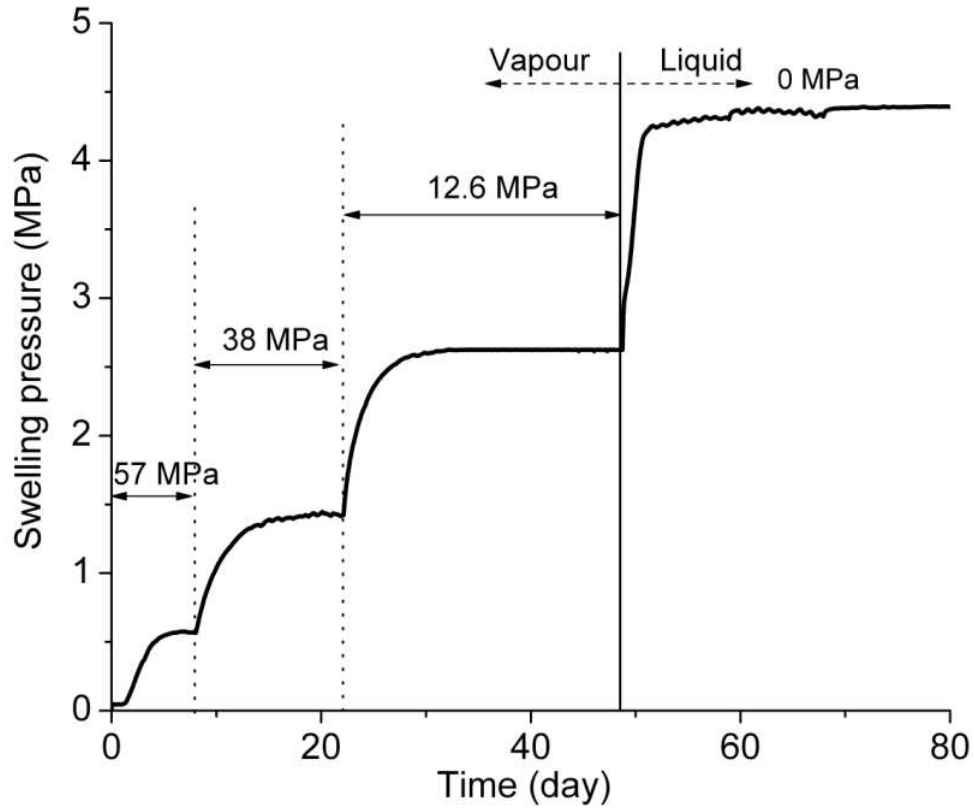Figure 5. Evolution of swelling pressure for test CV01 and CV02 during the first 100 h.

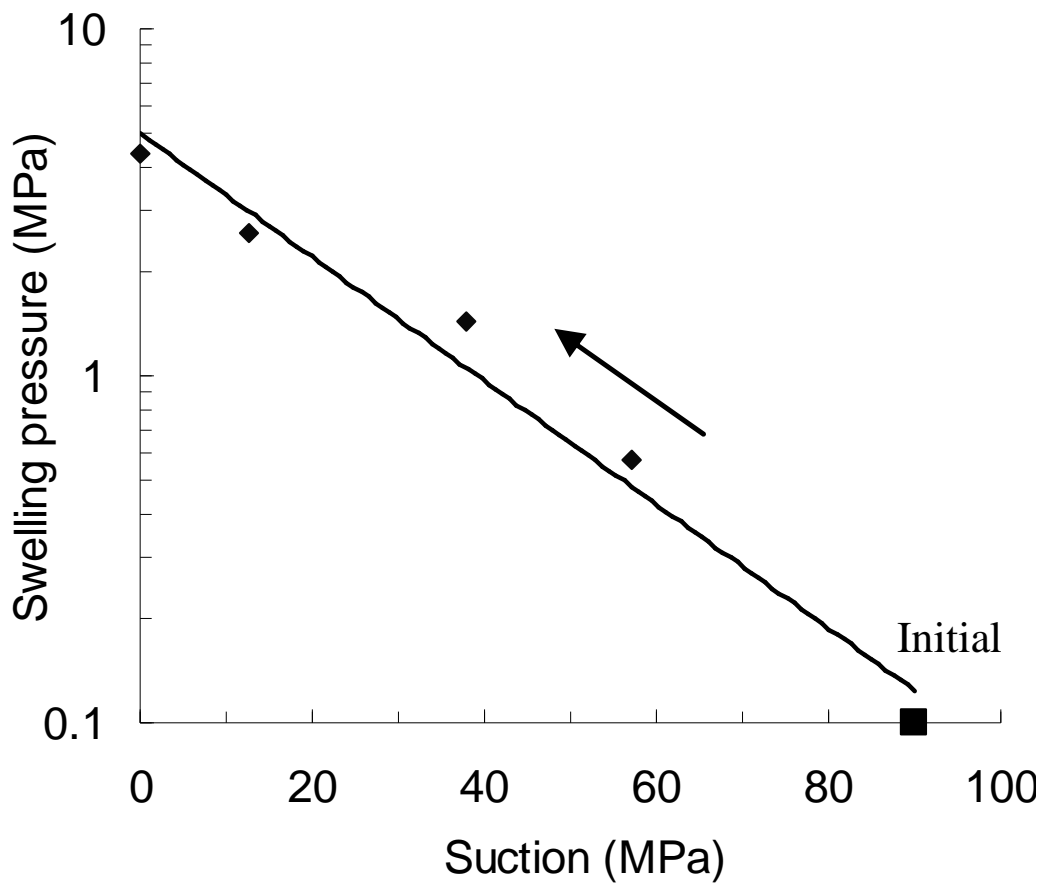Figure 6. Evolution of swelling pressure for test CV03 during decreasing of suction.

Figure 7. Swelling pressure versus suction of test CV03
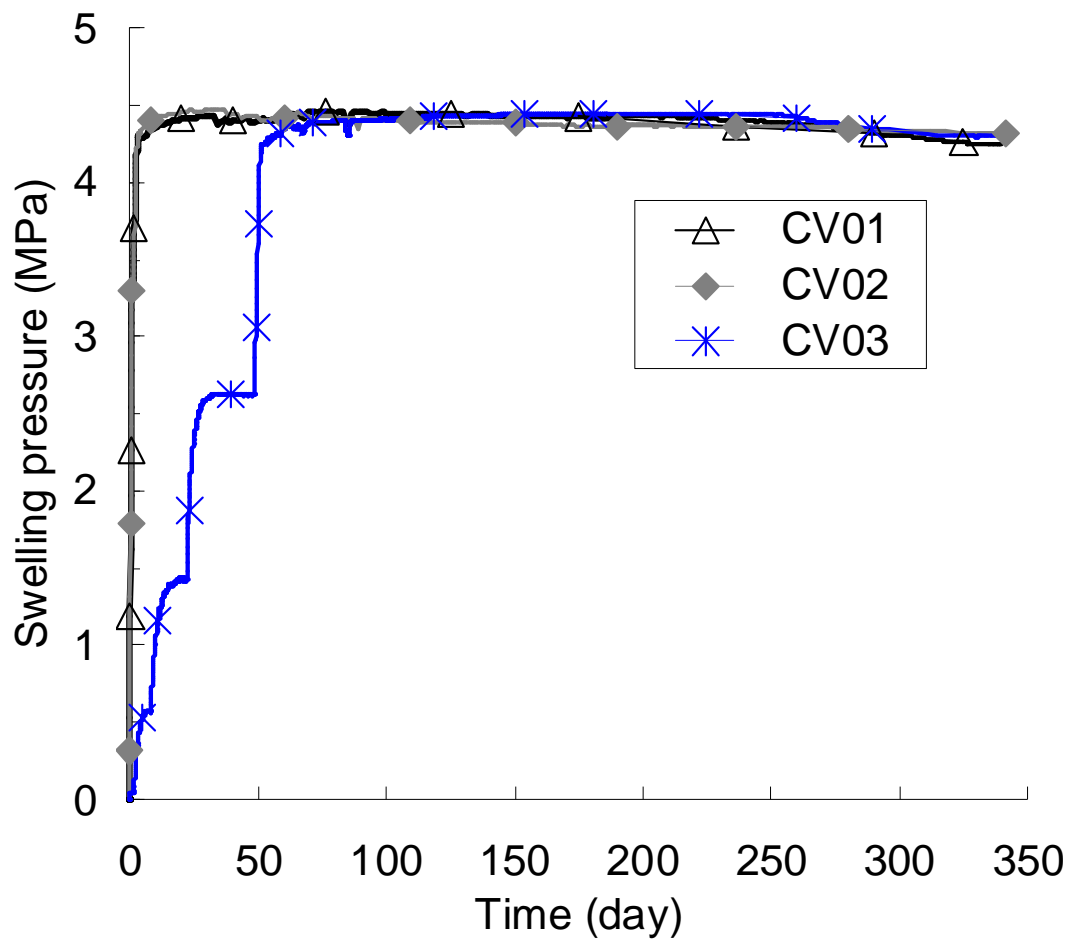
Figure 8. Evolution of swelling pressure for tests CV01, CV02, and CV03 for 1 year
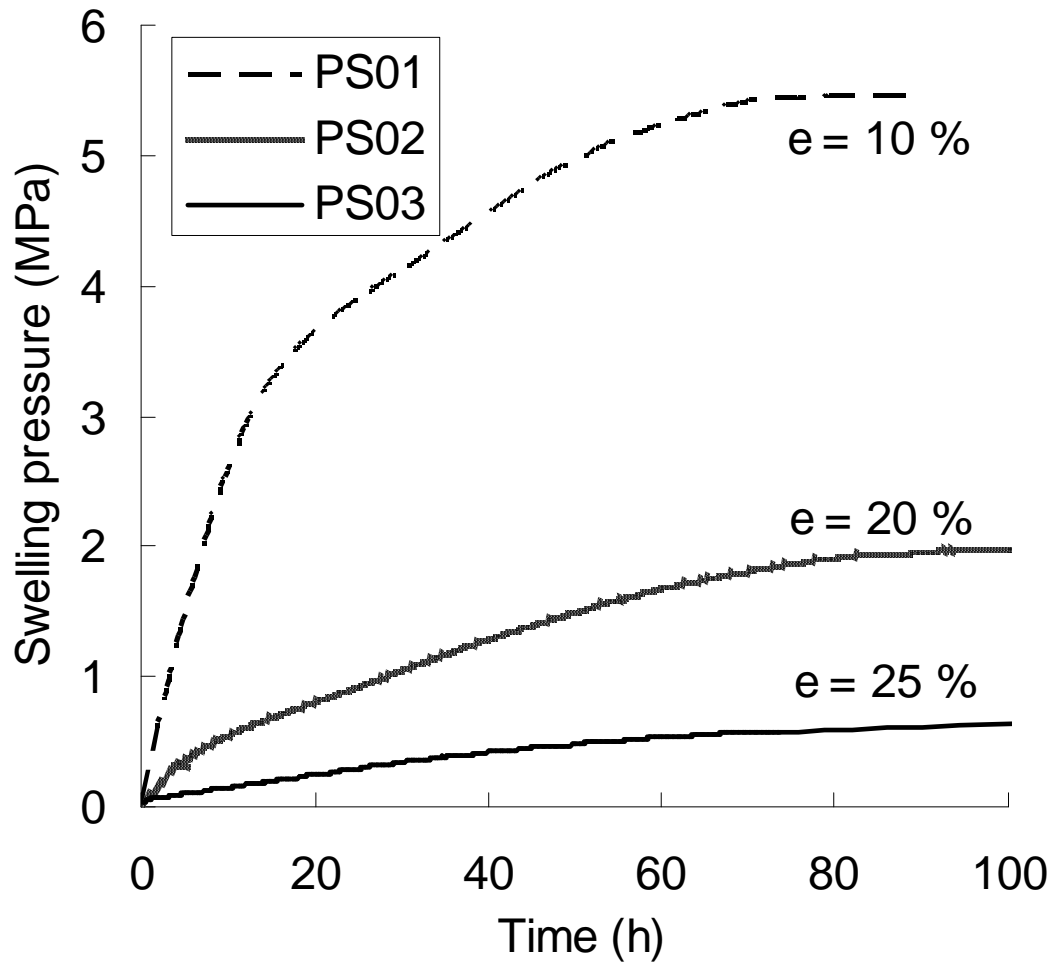
Figure 9. Evolution of swelling pressure with various pre-swells
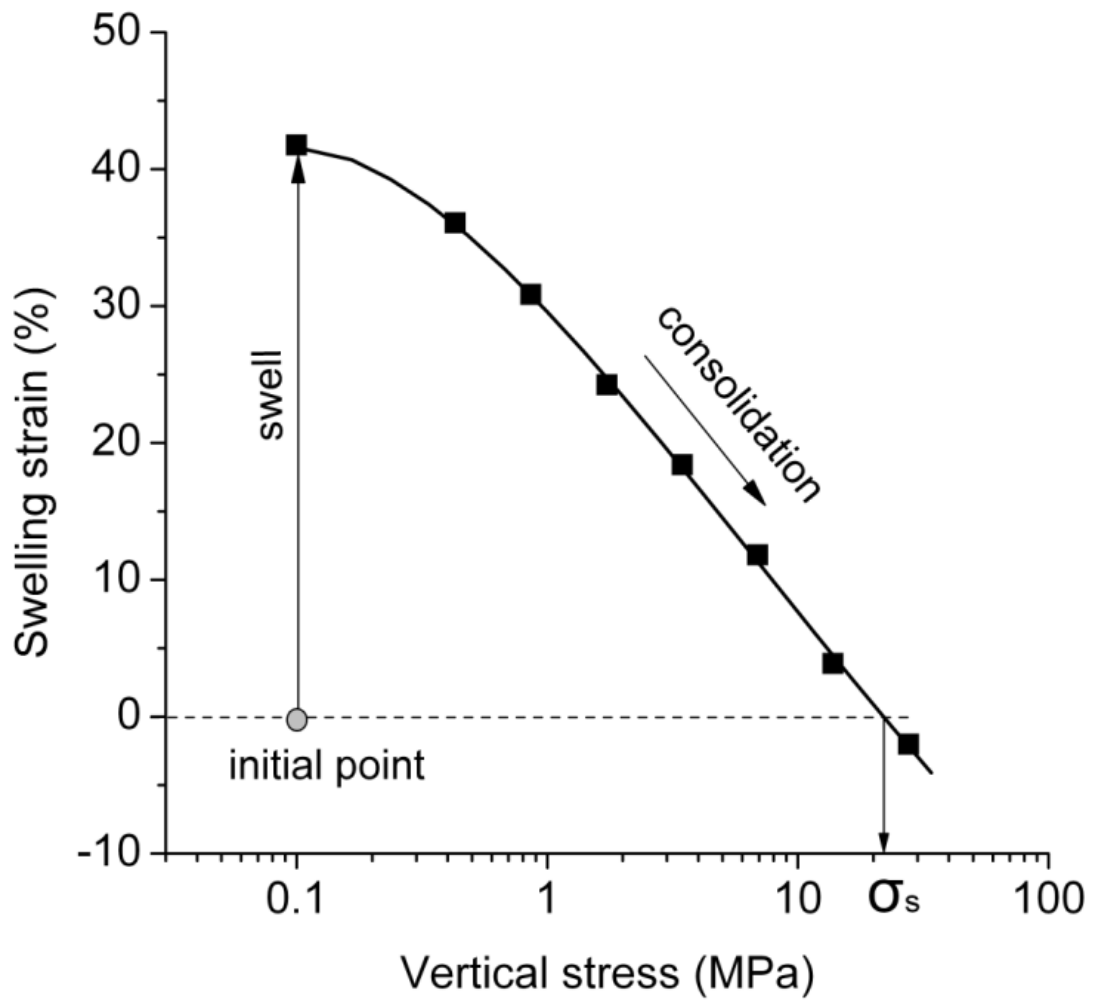
Figure 10. Swelling strain versus vertical stress applied for test SCO1
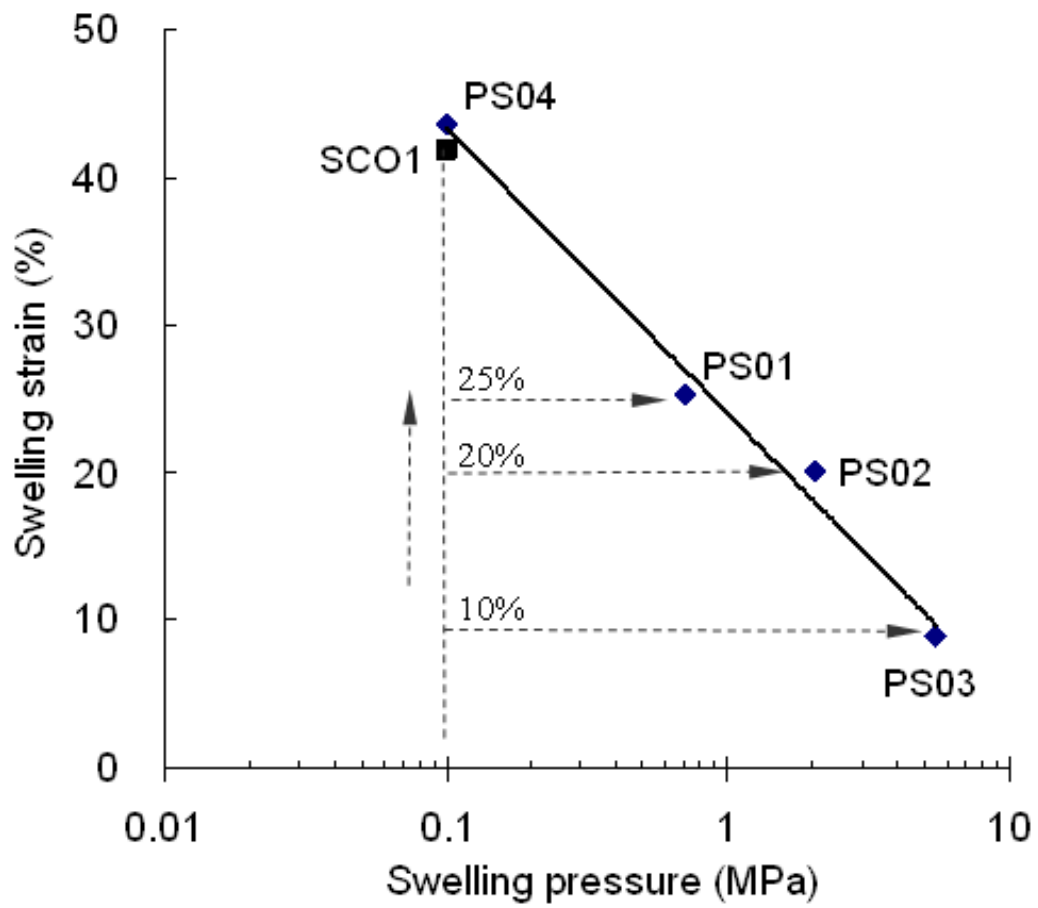
Figure 11. Pre-swell versus swelling pressure
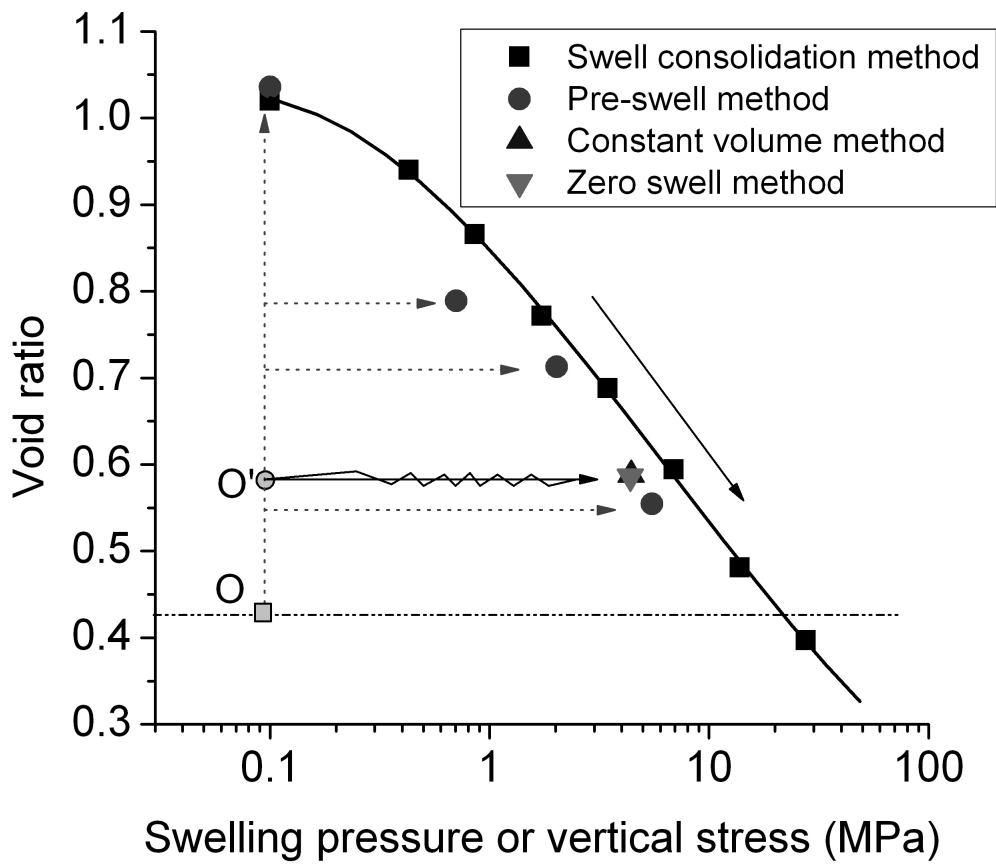
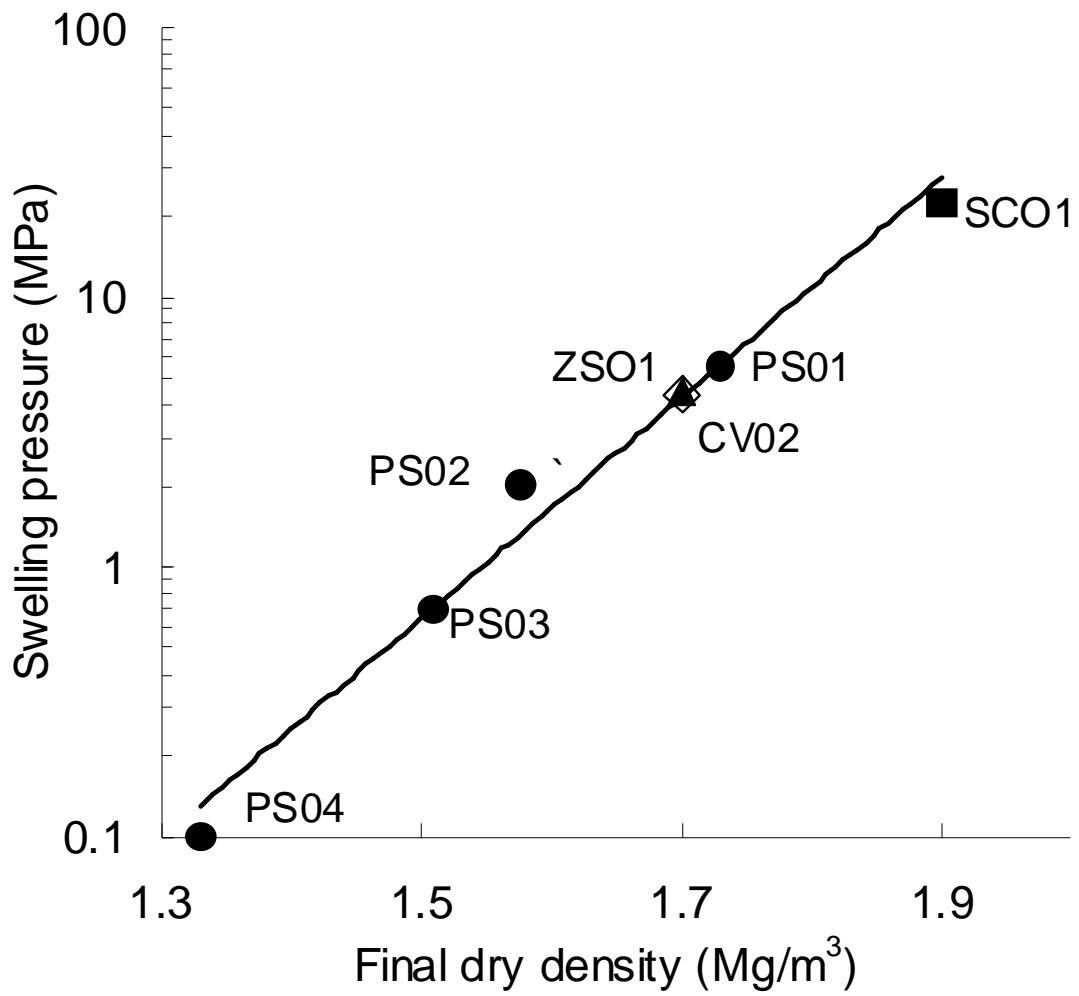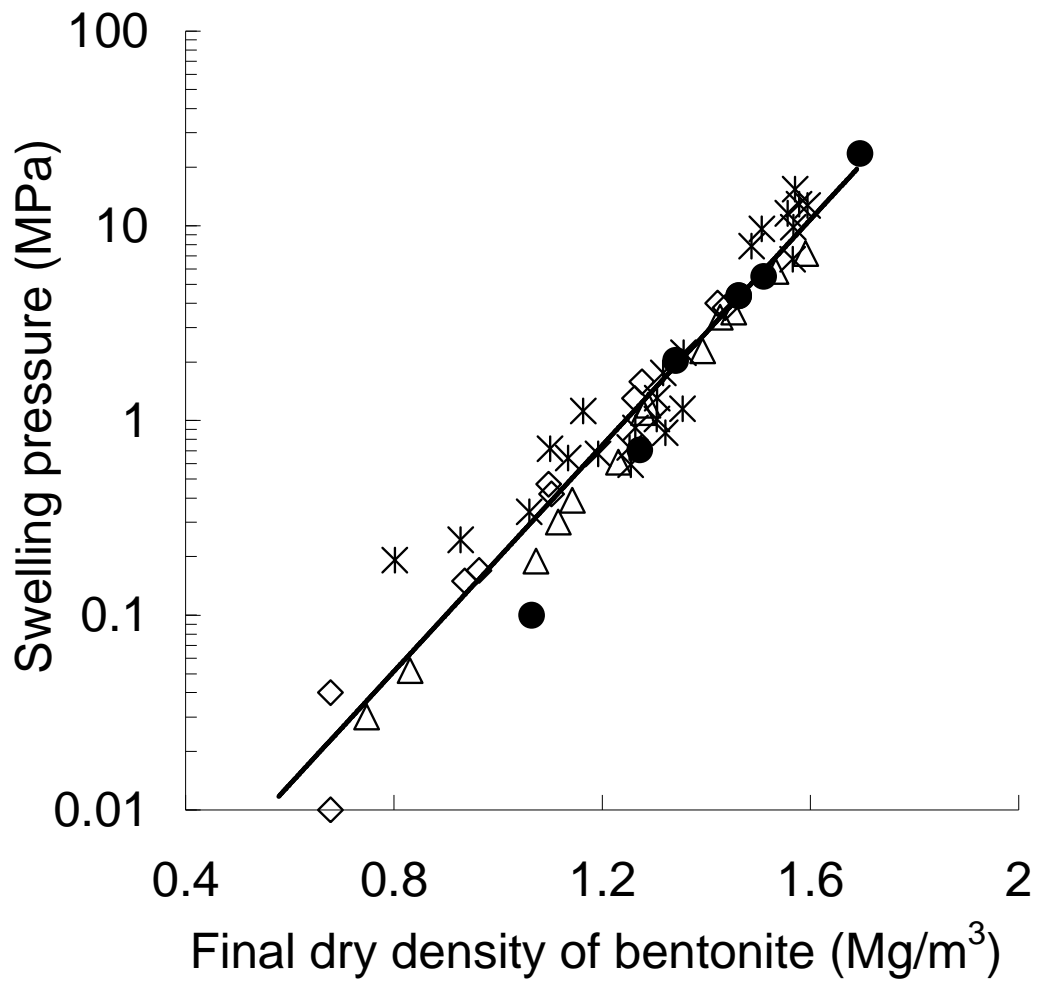Figure 12. Swelling pressure or vertical pressure versus void ratio of mixture

Figure 13. Swelling pressure versus finial dry density of bentonite/claystone mixture

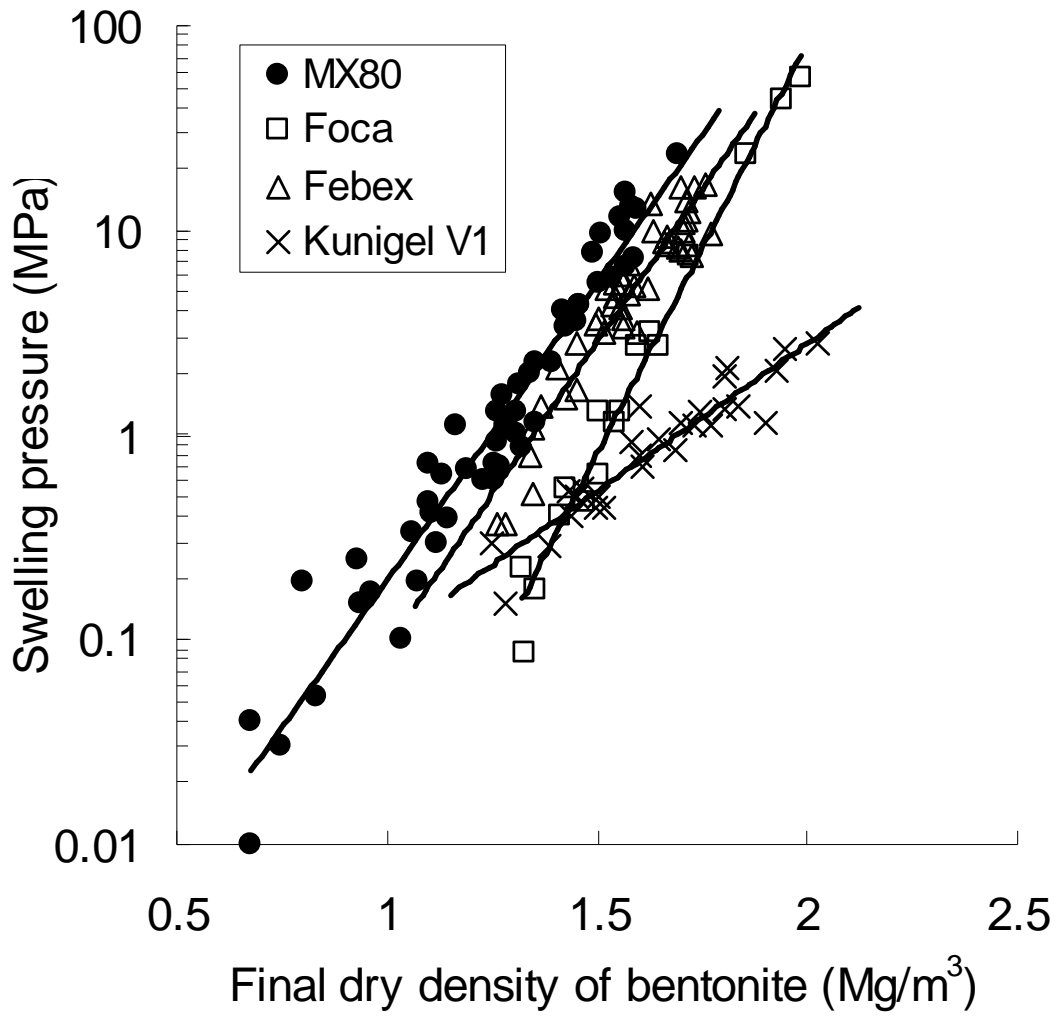Figure 14. Results of various mixtures using MX80 bentonite - swelling pressure versus final dry density of bentonite

Figure 15. Swelling pressure versus final dry density of bentonite